Diffusion exchange NMR spectroscopic study of dextran exchange through polyelectrolyte multilayer capsules

Y. Qiao and P. Galvosas
MacDiarmid Institute for Advanced Materials and Nanotechnology, School of Chemical and Physical Sciences, Victoria University of Wellington, Wellington, New Zealand

T. Adalsteinsson and M. Schönhoff
Institut für Physikalische Chemie, Westfälische Wilhelms-Universität Munster, Corrensstr. 30, D-48149 Münster, Germany

P. T. Callaghan[a)]
MacDiarmid Institute for Advanced Materials and Nanotechnology, School of Chemical and Physical Sciences, Victoria University of Wellington, Wellington, New Zealand

(Received 8 March 2005; accepted 6 April 2005; published online 6 June 2005)

Diffusion exchange of dextran with molecular weights 4.4 and 77 kDa through polyelectrolyte multilayer (PEM) hollow capsules consisting of four bilayers of polystyrene sulfonate/polydiallyldimethylammonium chloride has been investigated using two-dimensional nuclear-magnetic-resonance methods: diffusion–diffusion exchange spectroscopy (DEXSY) and diffusion–relaxation correlation spectroscopy (DRCOSY). Results obtained in DRCOSY experiments show that the diffusion process of dextran 77 kDa exhibits an observation time dependence suggesting a diffusion behavior restricted by confinement. We find evidence for both single capsule and capsule aggregate states, with a partitioning of the 77-kDa dextran between the free and capsule states much larger than that suggested by volume fraction alone. Results from DEXSY experiments show that dextran 77 kDa is in diffusive exchange through the capsules with an exchange time of around 1 s. In contrast, the capsules have no detectable influence on the diffusion process of the dextran 4.4 kDa. This quantitative information may be used in designing PEM capsules as drug carriers. © *2005 American Institute of Physics*. [DOI: 10.1063/1.1924707]

I. INTRODUCTION

Release-tailored encapsulated drugs have a number of advantages over conventional drug forms. For example, they can prolong the time of activity, protect sensitive drugs from human immune system and deliver drug to a specific site in human body, etc.[1] Various microstructures such as liposomes, microgels, microemulsions, polymer micelles, and colloids have been widely employed as drug carriers.[1] Recently, a novel microencapsulation technology, based on layer-by-layer assembly of oppositely charged polyelectrolytes[2] onto dissolvable colloidal templates,[3,4] has been established. Unlike liposomes, the polyelectrolyte multilayer (PEM) microcapsules are tough, uniform in size, and with selective and tunable permeability.

This specific permeability of the capsule wall is of particular interest in the design of release-controlled drugs. Laser confocal images have shown 20-nm thick-walled polystyrene sulfonate/polyallylamine hydrochloride (PSS/PAH) capsules exclude PSS with a molecular weight bigger than 4.4 kDa, but are permeable to small ions and 6-carboxyfluorescein (6-CF).[5] Confocal images have also shown that the same type of capsule may be reversibly and sharply switched by tuning the pH value between an open ($pH<6$) and a closed ($pH>8$) state to dextran (75 and 2000 kDa) and Al particles.[6] Scanning force microscopy images have shown that holes up to 100-nm diameter are present on the capsule surface when exposed to acidic solution, and that after transferring the same capsule into an alkaline solution of pH 10 the holes disappear.[6] The imaging techniques provide direct evidence that the permeability of the capsule wall is sensitive to the molecular weight of the solvent molecules and is tunable by changing the pH value, however, more quantitative information on the time scales associated with movement of macromolecules through the walls and within the capsules is needed.

In order to directly determine the time scale of the exchange of macromolecules through the capsule wall and the mobility of macromolecules within different domains of the macromolecule/capsule dispersion, we apply diffusion exchange and correlation two-dimensional (2D) nuclear-magnetic-resonance (NMR) techniques to study the diffusion behavior of dextran of two very different molecular weights, 4.4 and 77 kDa, through four bilayer-thick (~20 nm, 520-nm diameter template) polystyrene sulfonate/polydiallyldimethylammonium chloride (PSS/PDADMAC) capsules. Dextran is a water-soluble, biopolysaccharide that may be formed using enzyme technology, is commercially available, and is currently used as drugs. Certain grades of dextran are used as blood plasma volume expanders, and iron-dextran is used to combat iron-deficiency anemia.

NMR techniques are often limited to volume samples

[a)]Electronic mail: paul.callaghan@vuw.ac.nz

due to intrinsic insensitivity. However, systems with microstructure have extremely large surface areas/volume ratios, enhancing NMR sensitivity on surface features and consequently, NMR has become a powerful tool in surface research.[7] NMR research on PEM capsules is limited. Existing investigations have focused on the formation of the PEMs on particles.[8–10] ^{1}H solid-state NMR investigation using magic angle spinning (MAS) has been used to directly observe charge complexation in the system PSS/PDADMAC, and has led to the conclusion that the structure of the PEMs is identical to that of the bulk PE complex.[8] ^{1}H NMR investigations using T_2 relaxation have shown for the system PSS/PDADMAC a linear increase of relaxation rate R_2 with the number of layers, reflecting a constant increase of the hydration water immobilization with the adsorption of each layer, consistent with the increase of the thickness of the multilayer.[9] For the system PSS/PAH, involving a weak polyelectrolyte, it is found that while adsorption of a positive layer leads to an increase of R_2, a decrease of R_2 is observed after the adsorption of a negative layer, suggesting that the internal water mobility is controlled by the sign of surface charge and is thus oscillating. It has been pointed out that this reversible swelling behavior can be due to uncompensated charges within the internal layers (i.e., not only the outer layer) of the multilayer assembly,[9] and that internal rearrangements are responsible for this behavior.[11]

In a recent paper, Adalsteinsson *et al.*[12] report on a pulsed-gradient spin-echo (PGSE) NMR study of dextran diffusion in the hollow capsule PSS/PDADMAC system. Their measurements showed clearly the existence of more than one diffusion coefficient, and a biexponential model was used to fit the spin-echo attenuation data. The two diffusion coefficients so obtained were ascribed to the free dextran and to the dextran confined in the capsules. By analyzing the intensities of these components, allowing for relaxation effects in the process, evidence was found for a considerable enhancement of the dextran concentration within the capsules, over and above what would be expected on an equal portioning based on volume fraction alone.

The work presented here considerably extends that study by using new types of measurements of diffusion and spin relaxation in the dextran, which allow for model-free analysis. Recently developed pulsed-gradient spin-echo (PGSE) 2D NMR techniques have significant advantages over their one-dimensional (1D) counterparts. Even though it is possible to determine, by 1D pulsed-field gradient (PFG) NMR methods, both the exchange time τ_{exch} and the probability distribution of spins undergoing an exchange process[13] diffusion–diffusion exchange spectroscopy (DEXSY)[14,15] allows a model-free approach that directly determines quantitative information about exchange processes for a given mixing time τ_m in a single 2D experiment. Similarly diffusion–relaxation correlation spectroscopy (DRCOSY)[16] may be used to directly correlate diffusion coefficients T_2 relaxation times of multiple phases in a single 2D experiment for a given diffusion observation time. Both DEXSY and DRCOSY make overlapping diffusion and relaxation rates in multicomponent systems more easily distinguished through

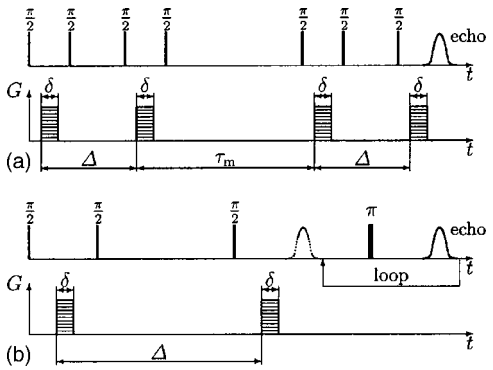

FIG. 1. (a) Diffusion exchange pulse sequence (DEXSY) based on two collinear pulsed-gradient stimulated-echo (PGSTE) sequences and separated by a mixing time τ_m. (b) Diffusion correlation pulse sequence (DRCOSY) combined a PGSTE and a multiecho sampling-type CPMG sequence.

separation in the second dimension. Furthermore, probability distributions for spins with each diffusion component may be determined.

The DEXSY[14,15] pulse sequence used here and shown in Fig. 1(a) consists of two pulsed-gradient stimulated-echo (PGSTE) sequences separated by a mixing time τ_m, in which the gradient pulse pairs may be changed independently. The resulting NMR signal as a function of the applied pulsed field gradients q_1 and q_2 is given by

$$M(q_1^2,q_2^2)/M_0 = \sum p(D_1,D_2)e^{-q_1^2 D_1 \Delta} e^{-q_2^2 D_2 \Delta}, \tag{1}$$

where M is the echo amplitude, M_0 is the initial echo amplitude, and p is the joint probability of the contribution to the signal from D_1 and D_2. $q=(\gamma G\delta)$, where γ, G, and δ are the gyromagnetic ratio, gradient strength, and gradient duration, respectively.

The DRCOSY pulse sequence shown in Fig. 1(b), consists of a combination of PGSTE and a multiecho sampling Carr–Purcell–Meiboom–Gill (CPMG) sequence.[17] The key difference in the current DRCOSY over that previous published[16] is that an echo train is acquired rather than a last echo in the CPMG part of the sequence. The advantage of this latest DRCOSY is that the experimental time may be greatly reduced, since the T_2 domain is sampled within one excitation through an echo train instead of carrying out the experiment many times while increasing the loop counter. As a result, the data need to be processed in the time domain instead of the frequency domain. The resulting signal is given by

$$M(t,q^2)/M_0 = \sum p(D,T_2)e^{-q^2 D\Delta} e^{-1/T_2}, \tag{2}$$

where p is the joint probability of the contribution to the signal from D and T_2.

The relationships expressed in Eqs. (1) and (2) are Laplace transformations from the p to M domains. In order to obtain p from M, inverse Laplace transformation is required. Such procedure for processing 2D NMR data has been introduced by Venkataramanan *et al.*[18] and Song *et al.*[19]

II. EXPERIMENT

The capsule stock solution was prepared following a protocol described earlier for the formation of multilayer-coated colloidal silica particles using a repeated adsorption–centrifugation method:[9,12] PDADMAC (M_w −100.000–150.000 g/mol) was purchased from Aldrich and used without further purification, while PSS (M_w =70.000 g/mol, Sigma) was purified by filtration, followed by lyophilization.

After the deposition of four bilayers of PSS/PDADMAC onto 520-nm diameter monodisperse colloidal silica (Geltech, Inc.), the silica core was dissolved: 10-ml dispersion of wt % of such coated colloids was added drop wise to 20-ml, 1.0-M HF solution while stirring for 40 min in centrifugation tubes to remove the silica cores. The sample was centrifuged at 4025 g (5000 rpm) for 30 min. 30-ml water was added after the HF acidic supernatant was removed and the above centrifugation process was repeated. After discarding the first water wash, the capsules were redispersed in 28-ml water and then, while stirring for 20 min, 2-ml 10-M HF was added. The samples were centrifuged, and the acid wash was discarded in excess $Ca(OH)_2$ solution. The capsules were then washed with water using centrifugation–decant–dilution cycles until the pH of the solution was around 5–6 and no CaF_2 formed when discarding the decanted liquid. Four samples prepared as above were combined and diluted to 20 ml. Assuming the density of silica is 2 mg/ml, the final concentration of capsule dispersion is maximum 1% v/v, which is the capsule stock solution.

Four NMR samples were prepared as follows. 3-ml capsule stock solutions were centrifuged in an Eppendorff vial at 2600 g (6525 rpm) for 15 min. After the supernatant was discarded, the capsules were redispersed in 99.95% isotope purity D_2O and the samples were centrifuged and the D_2O supernatant was discarded again. This D_2O wash was repeated for four times. Finally, the capsule dispersion was concentrated to 200 μl. 100-μl 10-mg/ml dextran in D_2O solution was added. In the final 300-μl sample, the volume ratio ϕ of capsules in D_2O is 10% v/v and the concentration of dextran in D_2O is 3.3 mg/ml. Two dextrans were employed as probe molecules: 4.4 and 77 kDa (Aldrich). In the further sections of this paper, these two NMR samples with capsules are referred as "dextran 4.4-kDa capsule dispersion" and "dextran 77-kDa capsule dispersion." Two other NMR samples are 3.3-mg/ml dextran in D_2O solutions and are referred as "dextran 4.4-kDa solution" and "dextran 77-kDa solution." These four NMR samples were transferred into 5-mm diameter NMR tubes.

High-resolution spectra of dextran of the above four NMR samples were obtained using a Varian300 NMR spectrometer. The spectra of dextran 77 kDa in (a) capsule dispersion and (b) dextran solution are shown in Fig. 2. The peaks between 3.3 and 4.2 ppm on the right-hand side of the H_2O peak (4.79 ppm, cut off at 3%) originating from protons at different sites of the dextran molecule are integrated and employed in the data analysis whenever data is required to be processed in frequency domain. The fact that there is no major difference between the spectra of the capsule dispersion and the pure dextran solution at the position between 3.3 and 4.2 ppm suggests that protons sited within capsule materials do not contribute to the NMR signals. However, the source of the largest contribution in the raw proton NMR spectra is HDO, which originates from the impurity of the D_2O solvent used for the sample preparation and/or from an exchange with the dextran protons. Note that the line broadening of the HDO signal caused by the capsules leads to a baseline contribution at the spectral position of the dextran molecules. In consequence, even when the signal is acquired from the spectral window of the dextran some water contribution remains and must be suppressed accordingly. The spectra for dextran 4.4 kDa are similar to the spectra of dextran 77 kDa, therefore, are not shown here.

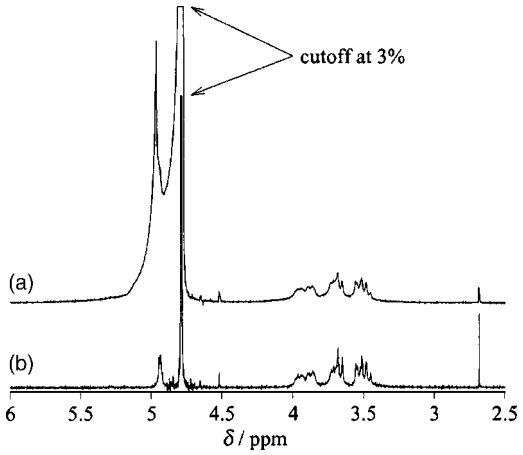

FIG. 2. High-resolution spectra of dextran 77 kDa in (a) hollow-capsule dispersion and (b) D_2O solution.

Diffusion experiments were performed using a Bruker AMX300 NMR spectrometer at a ^1H resonance frequency of 300.14 MHz at room temperature (22 °C). T_1 relaxation times of dextran for all samples were found to be around 1 s, and therefore, in the 1D diffusion experiments, the greatest Δ was chosen to be 500 ms. One-dimensional (1D) diffusion measurements were carried out using a Bruker Micro2.5 probe (maximum gradient strength $G_{\max}$=0.937 T/m), and employing a PGSTE pulse sequence over a series of Δ values. This gradient strength was sufficient for measurement of diffusion over times Δ in excess of 100 ms. The NMR signal was in the form of a free-induction decay (FID), which was Fourier transformed with the dextran peaks integrated in the frequency domain. The resulting intensities were subsequently treated with inverse Laplace transformation to yield the 1D distributions of diffusion coefficients.

For the DEXSY and DRCOSY experiments, where shorter values of Δ were used, a Bruker Diff60 probe ($G_{\max}$=36 T/m) was used. The maximum gradient employed was limited to 9.12 T/m. This higher gradient strength allowed us to fully attenuate the signal to zero, a significant advantage in subsequent data processing with the 2D inverse Laplace transformation. In order to avoid any possible influence of 50-Hz hum in the main power supply via the diffusion probe, the gradient amplifier was blanked during acquisition and observation times were only chosen as multiples of 20 ms between 60 and 300 ms. In the series of DRCOSY

experiments, measurements were performed in a random order of Δ to avoid any systematic drift of experimental conditions erroneously contributing to D vs Δ changes, for example, due to the settling of the hollow capsule into clusters in the sample within the experimental time. Data from DRCOSY measurements, which involved CPMG echo trains, were processed in time domain to obtain 2D matrices of signal intensities. During the inverse Laplace transformation, the signal from the very first few gradient steps was discarded in order to suppress any signal from water, which has a much higher diffusion coefficient than dextran. Note that the probability distributions present in final DRCOSY maps were corrected for T_2 decay by taking into account the calculable signal attenuation for that T_2 during the PGSTE part of the pulse sequence. In the two DEXSY experiments, Δ was chosen to be 60 ms.

In the DEXSY sequence [see Fig. 1(a)], the second gradient pairs are incremented first while the first gradient pairs are kept at a constant value; hence, after the inverse Laplace transformation, the vertical axis in the 2D DEXSY map represents the initial diffusion coefficient obtained by the first gradient pairs, while the horizontal axis stands for the final diffusion coefficient of the molecules measured by the second gradient pairs. By contrast with DRCOSY, where multi-CPMG echo trains are acquired, the NMR signals for DEXSY are acquired as FIDs, enabling subsequent Fourier transformation to the frequency (spectral) domain. This permits a spectral analysis so that the contribution of the water signal could be separated. However, as noted earlier even with the spectral selection at the position of the dextran peak a large contribution of the water "tail" appears in the NMR signal amplitude, leading in turn to a dominant peak ($>99\%$) in the 2D diffusion coefficient distribution. In order to investigate the dextran signal ($<1\%$) it was necessary to subtract the contribution of the water in the (q_1^2, q_2^2) domain prior to the 2D inverse Laplace transformation via

$$M_{\mathrm{corr}}(q_1^2, q_2^2) = M_{\mathrm{meas}}(q_1^2, q_2^2) - M_{\mathrm{water}} \exp(-q_1^2 D_{\mathrm{water}} \ddot{A}) \times \exp(-q_2^2 D_{\mathrm{water}} \ddot{A}), \quad (3)$$

where M_{meas} is the measured intensity in the 2D matrix in the (q_1^2, q_2^2) domain. D_{water} is the known diffusion coefficient of water, while M_{water} is adjusted until the disappearance of the diffusion peak corresponding to water in the final 2D diffusion distribution obtained in M_{corr}.

The areas under the dextran peaks in the spectrum could then be integrated, resulting in a 2D intensity matrix depending on q^2 in each domain. The contributions assigned to the peaks in 2D DEXSY maps are calculated from integrals of the volume under the surface of each peak in the 2D probability distributions. The experimental error in these probability distribution contributions is estimated to be 3%. Note, however, that this error represents only 0.03% of the total proton signal contribution, if the water contribution were to be included.

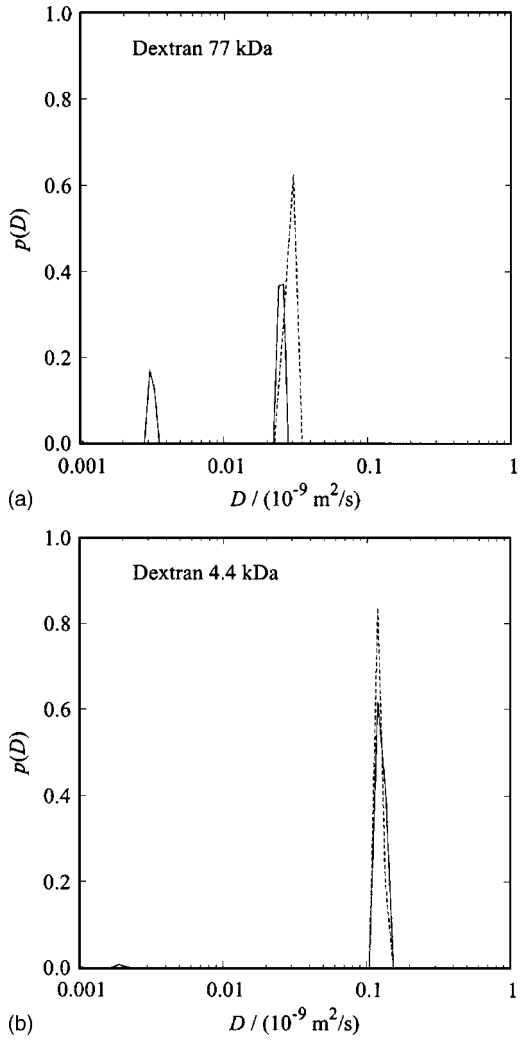

FIG. 3. Distributions of diffusion coefficients obtained though inverse Laplace transformation of the echo decays measured using PGSTE sequence, observation time at $\Delta = 100$ ms for both (a) dextran 77 kDa and (b) dextran 4.4 kDa samples. The solid lines stand for capsule dispersion samples and dashed lines stand for pure dextran solution samples.

III. RESULTS AND DISCUSSION

A. One-dimensional diffusion measurements

Figure 3 shows 1D distributions of dextran self-diffusion coefficients obtained by inverse Laplace transformation. These diffusion results were obtained using $\Delta = 100$ ms, with dashed lines for the dextran solutions and solid lines for the dextran capsule dispersions. It is clear that in the case of dextran 4.4 kDa, the presence of the capsules has no significant effect on the free diffusion of dextran. By contrast, for dextran 77 kDa, the presence of the capsules results in the appearance of a more slowly diffusing dextran component on the order of several 10^{-12} m^2/s. The diffusion coefficient of the fast component agrees, while the slow component is found to be higher as compared to the previous 1D results[12] [$(2.5 \pm 0.2) \times 10^{-11}$ m^2/s and 3×10^{-13} m^2/s, respectively]. However, this discrepancy arises from the fact that the diffusion coefficients reported here and in the previous work[12] does not characterize the same class of diffusing molecules, as we will show later. Moreover, the limitation of the gradient system used for the 1D PGSTE measurements affects

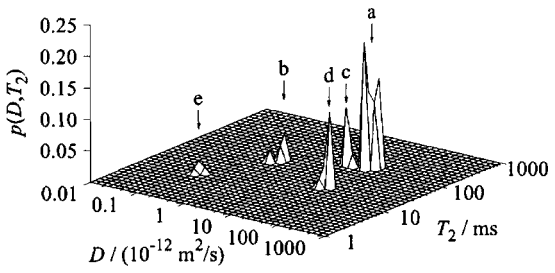

FIG. 4. A three-dimensional presentation of raw data obtained using DRCOSY pulse sequence after inverse Laplace treatment. The peaks stand for dextran with different diffusing behavior: (a) free-diffusing dextran in solution (D_{free}), (b) dextran confined inside capsules (D_{confined}), (c) dextran with a diffusion coefficient between the free-diffusing phase and the confined phase (D_{interact}), (d) free-diffusing dextran with a smaller T_2 relaxation time, and (e) dextran trapped inside hollow capsule clusters.

already the slow component by shifting it towards higher values, while fractions of the sample with even smaller diffusion coefficients do not appear at all in the distribution after the inverse Laplace transformation.

We shall argue that the capsule does not influence the diffusion process of dextran 4.4 kDa, presumably because of the free and rapid exchange of this small dextran between the bulk and the capsule interior, an effect we attribute to the much smaller size of the 4.4-kDa dextran by comparison with the capsule pore size. By contrast we argue that dextran 77 kDa, on entering the capsule, may be confined sufficiently for a distinctly slower diffusing component to be seen. The remainder of this paper concerns only the 77-kDa system.

B. Relaxation–diffusion correlation: 2D DRCOSY

An example of a three-dimensional presentation of the raw data obtained in a DRCOSY experiment, after inverse Laplace treatment, is shown in Fig. 4. The sample is the dextran 77-kDa capsule dispersion, and the result is obtained at $\Delta = 100$ ms. A number of peaks are labeled in Fig. 4. Peaks (a) and (d) correspond to a diffusion coefficient of free dextran. The differing T_2 values may be attributed to different sites on the dextran with (d) being a short relaxation time site, visible only for the free dextran. In order to make quantitative comparisons of the partitioning of the dextran between the free and confined states, and to avoid overestimating the total signal intensity in the free dextran fraction, we omit site (d) from all subsequent analysis. The power of DRCOSY is that it allows such discrimination. For all slower diffusing states of the dextran a single T_2 only is observed, a component we associate with the slowest relaxing proton site, i.e., site (a) of the free dextran.

Peak (b), as we shall show, corresponds to a diffusion coefficient similar to that expected for a freely diffusing capsule. Peak (c) arises from dextran diffusing a little more slowly than the free state, while peak (e) may arise from dextran trapped inside hollow capsule clusters. Our interpretation therefore is that the principal peaks correspond to dextran proton signals arising from (a) freely diffusing 77-kDa dextran in the bulk solution, (b) 77-kDa dextran confined inside single capsules, (c) 77-kDa dextran which has interacted with the capsule outer surface at an exchange time scale shorter than Δ (we call this the "fast surface-interacted phase"), and (e) 77-kDa dextran confined inside capsule aggregates. Peaks (a), (b), (c), and (e) all correspond to a site on the dextran molecule with the longest relaxation time, i.e., the site for which the free dextran T_2 relaxation time is around 120 ms, and for which a relaxation time of 113 ms was determined before.[12] Now, with the 2D methods, however, far more detail about the molecular behavior of this site is obtained.

The region encompassing peaks (a), (b), (c), and (e) is displayed in Fig. 5. We argue that these peaks arise from a common dextran site (based on the maximum value of T_2), but for different dextran molecular behaviors. Note, as mentioned in the Experiment section, the probability distributions have been processed to correct for the local T_2 decay, which results from the gradient-encoding period associated with the PGSTE part of the 2D pulse sequence. Figure 6 shows dependence on diffusion observation time Δ of DRCOSY results obtained using the dextran 77-kDa capsule dispersion. As Δ increases, peaks (a) and (c) retain constant diffusion coefficients, while peak (b), the confined phase, shifts to smaller D values. This is in agreement with the assignment that (a) and (c) result from freely diffusing molecules, while (b) represents a molecule in confinement. Further discussion will follow below. In the case of peak (e) the data are less conclusive, but does suggest a decreasing dependence of D as Δ increases. The diffusion coefficients of each phase agree with results obtained in 1D PGSTE experiments in Fig. 3(a).

Finally, similar DRCOSY experiments were carried out using the dextran 4.4-kDa capsule dispersion. In contrast to the above findings, no confined phase is observed, which is in agreement with the 1D PGSTE results in Fig. 3(b).

C. Interpretation of dextran diffusion

We now consider the specific values of the diffusion coefficients of dextran 77 kDa in the capsule dispersion, as shown in Fig. 5 and presented as a function of Δ in Fig. 6. The diffusion coefficients at around 2.5×10^{-11} m^2/s, associated with the freely diffusing dextran [peak (a)], are constant for Δ between 60 and 300 ms. This time independence is indeed consistent with the idea of freely diffusing molecules in the bulk. We henceforth refer to this diffusion coefficient as D_{free}. By contrast, the group of diffusion coefficients associated with peak (b) decreases from 1.6×10^{-12} to 6×10^{-13} m^2/s when Δ increases from 60 to 200 ms. Before discussing this downward trend, we focus on the absolute value of the diffusion coefficient, which we refer to as D_{confined}. Using the equation $R_H = k_B T/6\pi\eta D$ and $D_{\text{confined}} = 1.6\times10^{-12}$ m^2/s, the hydrodynamic radius R_{H} associated with the dextran is estimated to be 140 nm. We might have expected this value to be similar to that of the capsule, if peak (b) arises from intracapsule dextran. In fact the radius of colloidal silica particle used as a template is 260 nm. This discrepancy could be due to the fact that the shape of a hollow capsule in solution is irregular (see images in Refs. 3 and 5). Furthermore, the capsule (unlike the silica template) is highly porous to the solvent water molecules, reducing the effective Stokes radius. Thus we would argue that the evi-

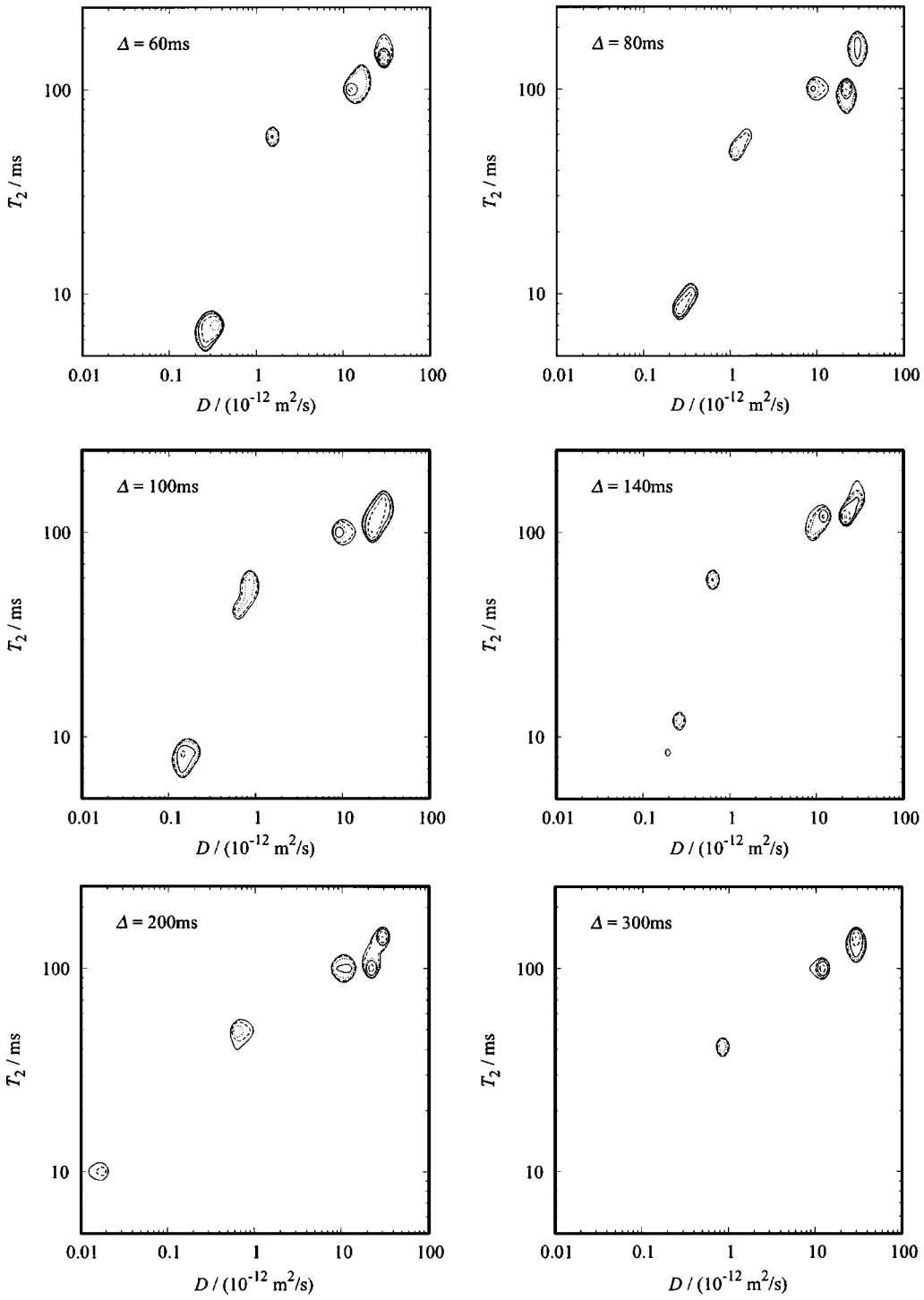

FIG. 5. Results obtained using DRCOSY in dextran 77-kDa capsule solution measured at six different observation times. The isolines are 3% (—), 6% (– – –), 12% (·····), 25% (—), 50% (– – –), and 100% (·····). The highest peak in each figure is normalized to 100%.

dence is consistent with peak (b) arising from the intracapsule state. Note that the T_2 relaxation time associated with this group of diffusion coefficients is about 52 ms, which is smaller than T_2 of the free-diffusing dextran (120 ms), most probably due to the influence of the confinement.

The declining value of D_{confined} as Δ increases between 60 and 300 ms is easily understood. Using the known volume ratio of capsules (10%) and the template radius of 260 nm, we may estimate the spacing between capsules in the dispersion as around 390 nm. Using $\langle z^2 \rangle = 2D\Delta$ and $D_{\text{confined}} = 1.6 \times 10^{-12}$ m^2/s, the square root of mean-square displacement is estimated to be 440 nm at $\Delta = 60$ ms and, of course, greater at longer times. This diffusion distance is similar to or greater than the typical spacing between capsules. With increasing diffusion length, the number of interparticle collisions increase and the effective diffusion coefficient is reduced to an asymptotic value for D_{confined}, as described by the free-volume theory.

Turning our attention to peak (c), we note that the dextran, with diffusion coefficients at around 1.1×10^{-11} m^2/s

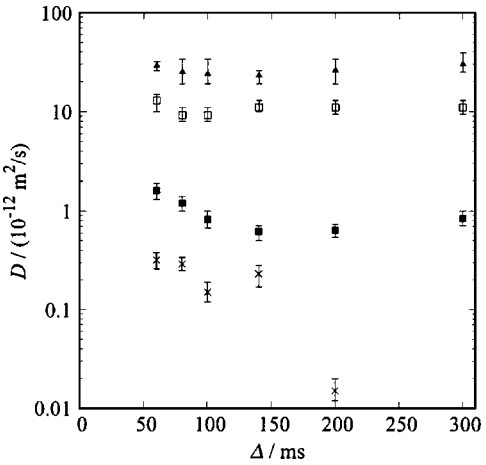

FIG. 6. D vs Δ results obtained using DRCOSY after inverse Laplace treatment. The same results in 2D graphs are presented in Fig. 5. The points are free dextran [peak (a)] (▲) interacting dextran [peak (c)] (□), dextran confined to single capsules [peak (b)] (■), and dextran confined to capsule aggregates [peak (e)] (×).

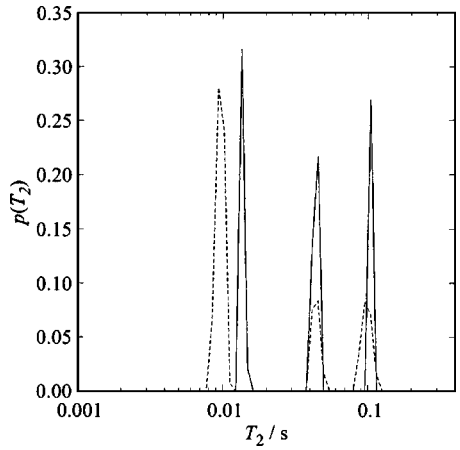

FIG. 7. Probability distributions of T_2 obtained in a one-dimensional CPMG experiment with water suppression by means of a preceding PGSTE gradient pulsed pair on 77-kDa dextran in the capsule solution. The solid lines correspond to measurements immediately after sonication, while the dashed lines are for 17 h later.

and constant for Δ between 60 and 300 ms, have D values between D_{free} and D_{confined}. However, it is easy to show that such a value cannot be the average of the free and confined phases and cannot therefore arise from dextran in fast exchange. Using $D_{\text{confined}}=1.6\times10^{-12}$ m^2/s, $D_{\text{free}}2.5\times10^{-11}$ m^2/s, and $\phi=10\%$, D_{average} is estimated as 2.3×10^{-11} m^2/s. An alternative explanation for this reduced diffusion coefficient is that some dextran molecules may diffuse around the capsules, but do not directly enter the capsule. We postulate that the dextran temporarily interacts with the outer surface of the capsules, on a timescale that is shorter than the observation times (60 to 300 ms), within that timescale leaving the capsule surface and joining the free-diffusing dextran. We present this diffusion coefficient as D_{interact}. The T_2 for such dextran is around 100 ms, smaller than that of the free dextran (120 ms), and consistent with the idea that the fast transient interaction could be a mechanism that slightly reduces the rotational mobility of dextran, as well as its translational mobility.

Finally, we consider peak (e) with associated diffusion coefficients falling in the range 3.2×10^{-13}–1.7×10^{-14} m^2/s and with T_2 values on the order of 10 ms. This much slower diffusion coefficient is most likely to arise from dextran confined in capsule aggregates. Further, we find that the diffusion coefficients exhibit some variation depending on the time after sonication at which measurement was performed. We also observed some variation of D values in component (e) with the age of the sample. The time dependence is also apparent in T_2 measurements (carried out with suppression of the water signal utilizing a gradient pulse pair of a fixed amplitude prior to the CPMG echo train) shown in Fig. 7. Here we see a distinct downwards shift in the 10-ms component, associated with peak (e), when the measurement is performed 17 h after sonication. We take this as evidence for aggregation development over this time.

A noticeable aspect of component (e) in the vicinity of $T_2=10$ ms and $D\sim10^{-13}$ m^2/s, in Fig. 5, is the significant drop in intensity as the encoding time Δ is increased, as can be seen by inspection of Fig. 5. In the PGSTE encoding used to measure diffusion, Δ corresponds to a period of "z storage" during which T_1 relaxation occurs. One obvious explanation of the relative reduction of intensity with increasing Δ is the more rapid T_1 relaxation for component (e). In support of that assertion we show in Fig. 8 the intensities (T_2 corrected) for peaks (a), (b), (c), and (e) plotted against the storage time $\Delta-\tau_1$, τ_1 being the "T_2-susceptible" period during which magnetization resides in the transverse plane and for which intensity loss has been corrected using the known T_2 values taken from Fig. 5. Figure 8 suggests that peaks (a), (b), and (c) have T_1 relaxation times on the order of 300 ms, while peak (e) has 32 ms$<T_1<$45 ms. The faster T_1 relaxation in this site can be caused by dextran chains entangled between aggregated capsules, such that their fast, local segment motions, which dominate T_1, are hindered.

Figure 8 permits us to correct for T_1 relaxation effects, so as to obtain a relative intensity for all peaks for which all relaxation effects (T_1 and T_2) have been removed. We find

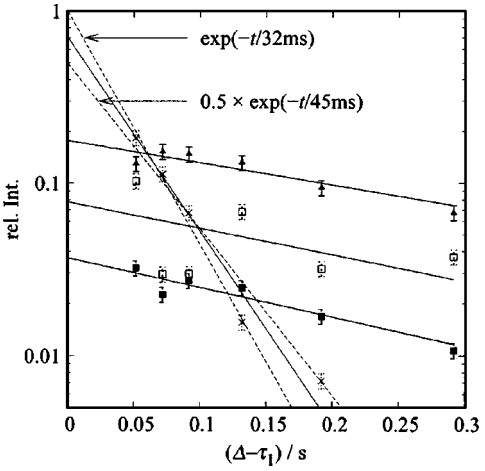

FIG. 8. Relative intensities of dextran peaks as a function of "z-storage time," but with T_2 corrections already made. The decays show evidence of T_1 relaxation. The points are free dextran [peak (a)] (▲), interacting dextran [peak (c)] (□), dextran confined to single capsules [peak (b)] (■), and dextran confined to capsule aggregates [peak (c)] (X).

respective proportions: free dextran [peak (a)] 0.18 ± 0.02, interacting free dextran [peak (c)] 0.08 ± 0.04, dextran confined to single capsules [peak (b)] 0.037 ± 0.004, and dextran confined to capsule aggregates [peak (e)] 0.7 ± 0.2. Grouping together the free dextran $[(a)+(c)]$ and the confined capsule dextran $[(b)+(e)]$, we deduce a partitioning enhancement factor, over and above that suggested by the 10% capsule volume fraction, or around 30. This factor is one order of magnitude larger than that estimated by Adalsteinsson *et al.*[12] We attribute this different finding to the fact that we have, as required by a consistent comparison, excluded the peak (d) from the analysis, since this peak arises from a free-dextran site not observed in the other dextran dynamical states. By this exclusion we ensure that we do not overestimate the amount of free dextran. Nonetheless, we add the *caveat* that the partitioning-enhancement factor may well depend on the degree of aggregation and it is possible that aggregation may have been different in the two experiments. By the large relative population of peak (e), this fraction strongly depends on the degree of aggregation of capsules.

D. The diffusion exchange process: 2D DEXSY

Figure 9 shows the results of DEXSY measurements obtained using dextran 77-kDa capsule dispersion at mixing times τ_m of (a) 20 and (b) 200 ms. The diffusion coefficient range encompassed corresponds only to peaks (a), (b), and (c), so that we will restrict our attention to dextran exchanging between single capsule and free states. We focus first on the dominant diagonal part of the spectrum, corresponding to dextrans which have not changed their dynamical state over the mixing period. First, we note the good correspondence of the magnitude of slow- and fast-diffusion components with those obtained in the DRCOSY and PGSTE experiments. Second, we turn our attention to the quantitative analysis of peak areas (again T_2 corrected). In Fig. 9(a), the area corresponding to dextrans which diffuse freely or nearly free outside the capsules is 90.5%, while 9.5% of dextran appear to diffuse at a rate close to the capsule value. Note that these numbers represent relative occupancies of the free and single capsule states, but are not absolute intensities since we omit the intense aggregate capsule state in this DEXSY analysis. However, the signal intensity ratios of the two diagonal peaks in Fig. 9(a) agree with the corresponding intensities extracted from Fig. 8. In Fig. 9(b), the two diagonal peaks again correspond in their intensities to expected values. However, at this longer mixing time of 200 ms, distinct off-diagonal peaks appear, with integrated probability intensities of 3.0% and 0.2%.

The presence of off-diagonal features in a DEXSY experiment provides a clear evidence of exchange. We argue that these off-diagonal features originate from the dextran molecules moving between the capsule and the bulk over the mixing time. Although the error is still 3%, we present data to a precision of 0.1% in order to retain all four peaks with intensities 86.8%, 10.0%, 3.0%, and 0.2%. Of course, dynamic equilibrium requires that the intensities of off-diagonal peaks are identical. The apparent unbalance of the intensities indicated here is a consequence of the error. It is worth remarking, in mitigation, that the absolute error in our intensities is very small, the two exchange peaks representing only 0.01% of the total NMR signal, which contributes to the intensities of the exchange peaks. We are, in fact, investigating a very delicate effect. Given that symmetry demands equal off-diagonal intensity, we take that intensity to be the mean value ~1.5%.

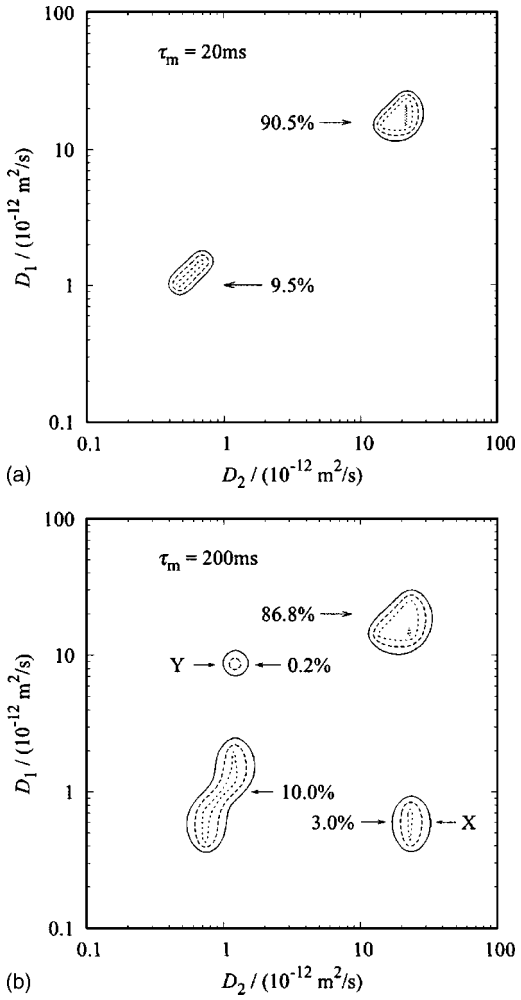

FIG. 9. Diffusion exchange results obtained using DEXSY pulse sequence in which (a) $\tau_m=20$ ms and (b) $\tau_m=200$ ms. The probability distributions of spins are calculated by integrating the corresponding peaks in three-dimensional diagrams with an experimental error of 3%.

By contrast, the asymmetry of the positions of the exchange peaks may not arise from the experimental uncertainty effect and is discussed here in the context of our model. We propose that molecules, which enter the dextran capsule during the mixing time, came from the population of dextran involved in temporary surface interactions, and thus originating from a diffusion coefficient state slightly reduced from the bulk phase. We further propose that the dextran that escapes the capsule, escapes freely into the bulk. In fact, phase (c) may exchange to phase (b), but phase (b) exchanges back not to phase (c) but to phase (a). The exchange between phases (a) and (c) retains the required dynamic balance, but is not easily seen on the DEXSY plot because of the close diagonal proximity of phases (a) and (c).

Thus we argue that the off-diagonal peak X (nominal intensity 3.0%) arises from dextran starting with D_{confined} and

ending directly with D_{free}. The peak Y (nominal intensity 0.2%) arises from dextran starting with D_{interact} and ending with D_{confined}. This model is consistent with the idea that the dextran inside the capsules may directly eject out of the capsule, but only the dextran that are already being temporarily interacting with the capsule surface may enter the capsules. Finally, we note that since no exchange is evident at a mixing time of 20 ms, but around 1.5% exchange occurs at 200 ms, the exchange time for this process must be on the order of several hundred milliseconds. When complete exchange occurs the off-diagonal peaks should have an intensity of $\sim$10%, a value which reflects the equilibrium distribution of dextran probability between the capsule and free states. Assuming an exponential process, we may estimate $\tau_{\text{exchange}} \sim 1$ s.

IV. CONCLUSION

Results obtained in PGSTE, DRCOSY, and DEXSY experiments show that a confined phase of dextran 77-kDa molecules is found in the dextran/capsule system, while in contrast, the same capsules have no detectable influence on the diffusion of the dextran 4.4-kDa molecules. The values of diffusion coefficients found are consistent with four states for the dextran: freely diffusing in the bulk, in transient interaction with the capsule surfaces, and confined both within the capsules and capsule aggregates, albeit with a slow exchange process to the exterior. In DRCOSY experiments, the dependence of diffusion coefficients on observation time suggests a restricted diffusion behavior of dextran 77-kDa molecules within the capsules as well as evidence for intercapsule interactions. The distributions of diffusion coefficients obtained in DEXSY experiments agree with results obtained in the PGSTE measurement and in the DRCOSY experiments.

We note here that the dextran confined to capsule aggregates dominates the overall 77-kDa dextran signal once relaxation effects are corrected. Further, we find that the 77-kDa dextrans are nearly 30 times more likely to be found in the single capsule and capsule aggregate states compared with an estimate based on volume fraction alone. This estimate is significantly higher than that made by Adalsteinssson *et al.*,[12] an effect we attribute to a more detailed relaxation analysis on our part, and our avoiding and overestimation of the free-dextran contribution through our noninclusion of the visible, but nonequivalent free-dextran proton sites.

About 1.5% of dextran 77-kDa molecules exchange through capsule walls between the confined phase and the free and surface-interacting phases at mixing times of 200 ms, suggesting an exchange time on the order of $\sim$1 s. The asymmetry of the exchange peaks in the DEXSY map may be tentatively interpreted in terms of a model whereby the dextran inside the capsule may escape directly to the bulk, but only the dextrans that are in transient interaction with the capsule surface may enter. The quantitative information on dextran exchange and diffusion found here prove useful in designing polyelectrolyte multilayer capsules for use as drug carriers.

ACKNOWLEDGMENTS

The authors are grateful to the New Zealand Foundation for Research, Science and Technology, the Royal Society of New Zealand Marsden Fund, and Centres of Research Excellence Fund for grant support.

[1] T. L. Whateley, *Macroencapsulation of Drugs* (Harwood, Academic, Amsterdam, 1992).
[2] G. Decher, Curr. Opin. Colloid Interface Sci. **277**, 1232 (1997); M. Schönhoff, Curr. Opin. Colloid Interface Sci. **8** (1), 86 (2003); M. Schönhoff, J. Phys.: Condens. Matter **15**, R1781 (2003).
[3] E. Donath, G. B. Sukhorukov, F. Caruso, S. A. Davis, and H. Möhwald, Angew. Chem., Int. Ed. **37**, 2202 (1998).
[4] G. B. Sukhorukov, E. Donath, H. Lichtenfeld, E. Knippel, M. Knippel, A. Budde, and H. Möhwald, Colloids Surf., A **137**, 253 (1998).
[5] G. B. Sukhorukov, M. Brumen, E. Donath, and H. Möhwald, J. Phys. Chem. B **103**, 6434 (1999).
[6] A. A. Antipov, G. B. Sukhorukov, S. Leporatti, I. L. Radtchenko, E. Donath, and H. Möhwald, Colloids Surf., A **198**, 535 (2002).
[7] M. Schönhoff, in *Novel Methods to Study Interface Layers*, edited by D. Möbius and R. Miller (Elsevier, Amsterdam, 2001), pp. 285.
[8] L. N. J. Rodriguez, S. M. De Paul, C. J. Barrett, L. Reven, and H. W. Spiess, Adv. Mater. (Weinheim, Ger.) **12**, 1934 (2000).
[9] B. Schwarz and M. Schönhoff, Langmuir **18**, 2964 (2002).
[10] B. Schwarz and M. Schönhoff, Colloids Surf., A **198**, 293 (2002); M. McCormick, R. N. Smith, R. Graf, C. J. Barrett, L. Reven, and H. W. Spiess, Macromolecules **36**, 3616 (2003); R. N. Smith, M. McCormick, C. J. Barrett, L. Reven, and H. W. Spiess, Macromolecules **37**, 4830 (2004).
[11] D. Carriere, R. Krastev, and M. Schönhoff, Langmuir **20**, 11465 (2004).
[12] T. Adalsteinsson, W. F. Dong, and M. Schönhoff, J. Phys. Chem. B **108**, 20056 (2004).
[13] J. Kärger, H. Pfeiffer, and W. Heink, Adv. Magn. Reson. **12**, 1 (1988).
[14] P. T. Callaghan and I. Furo, J. Chem. Phys. **120**, 4032 (2004).
[15] P. T. Callaghan and M. E. Komlosh, Magn. Reson. Chem. **40**, S15 (2002).
[16] S. Godefroy and P. T. Callaghan, Magn. Reson. Imaging **21**, 381 (2003).
[17] P. Galvosas, Y. Qiao, and P. T. Callaghan (unpublished).
[18] L. Venkataramanan, Y. Q. Song, and M. D. Hurlimann, IEEE Trans. Signal Process. **50**, 1017 (2002).
[19] Y. Q. Song, L. Venkataramanan, M. D. Hurlimann, M. Flaum, P. Frulla, and C. Straley, J. Magn. Reson. **154**, 261 (2002).